ELSEVIER

Journal of Structural Geology 26 (2004) 1913–1930

JOURNAL OF STRUCTURAL GEOLOGY

www.elsevier.com/locate/jsg

Growth pattern of underlithified strata during thrust-related folding

F. Nigro*, P. Renda

Dipartimento di Geologia e Geodesia dell'Università, C.so Tukory n. 131, 90134, Palermo, Italy

Received 1 November 2002; received in revised form 11 March 2004; accepted 18 March 2004

Available online 18 May 2004

Abstract

Asymmetric anticlines with overturned or steeply dipping forelimbs and gently dipping backlimbs are generally interpreted as thrust-related folds. Fold asymmetry occurs as a consequence of forelimb rotation. If deformation takes place in environments dominated by submarine sedimentation, the limbs coincide with the slope (depositional surface) and rotation reflects slope steepening. If folds are nucleated in poorly or unlithified deposits, growth geometry also depends on the properties of the media, such as cohesion and the angle of internal friction. For cohesionless deposits, the tilting of the slope influences the equilibrium of the soft sediments, resulting in gravity-driven flow, re-mobilisation or in situ compaction. The occurrence of mass re-mobilisation is also connected with the limb tilting/lithification ratio. Hence, the presence of non-primary bedding geometries or soft-sediment deformations in folding-related growth strata may provide useful tools for deciphering contractional kinematics.

Deformation of underlithified sediments during thrust-related folding is recorded in the outer sector of the Neogene Sicily chain (Central Mediterranean). Deformation occurred during the building of the Pliocene chain. Folding is the driving mechanism of the growth stratal pattern. Fold nucleation and amplification influenced the inclination of the slope of the basin floor where sediments were deposited. Slump and stretching structures in soft sediment occurred during folding and mass accumulation at the base of limbs led to a decrease in slope inclination. Analysis of fault-related fold and gravity-driven geometries enable us to reconstruct the contractional kinematics and the behaviour of syn-tectonic deposits that modify the growth fold pattern in terms of limb-hinge change of length-thickness.

Keywords: Soft-sediment deformations; Stratal pattern; Fold growth; Thrust tectonics; Pliocene; Sicily

1. Introduction

The geometric relationships between fold growth and related syn-tectonic stratal pattern are largely understood for fault-related folds (Medwedeff, 1989; Suppe et al., 1992, 1997; Zoetemeijer et al., 1992; Hardy and Poblet, 1995; Hardy et al., 1995; Torrente and Kligfield, 1995; Zapata and Allmendinger, 1996; Ford et al., 1997; Storti and Poblet, 1997).

During thrust-related folding, different stratal patterns develop in the forelimb, backlimb and hinge regions (Medwedeff, 1989; Suppe et al., 1992; Shaw and Suppe, 1994).

Folding and thrusting rates have been determined using growth strata analysis by Suppe et al. (1992), who consider asymmetric fold amplification as related to kink-band migration towards the foreland in the case of invariance of limb inclination during fold amplification. Torrente and Kligfield (1995) describe the relationships between the growth of low-amplitude buckle folds and the associated syn-tectonic sedimentation. The influence of several factors (such as fold uplifting, limb rotation/widening rates, sedimentation/erosion rates) on growth stratal geometries has been examined by Storti and Poblet (1997) for décollement and fault-propagation folding.

Nevertheless, the general folding-related growth strata modelling does not always take into account the lithological characteristics or the degree of lithification during deformation, which may influence the final stratal pattern in depositional settings dominated by tectonics.

'Soft-sediments' and 'hard-rocks' may be deformed both by tectonic processes and under the influence of gravity (Maltman, 1984). Fold and fault geometries deriving from downslope translation of unlithified sediments are analogous to tectonic structures (Woodcock, 1976; Tobisch, 1984) and may be easily mistaken for these.

Soft-sediment deformations are commonly interpreted as

* Corresponding author. Tel.: +39-91-7041013; fax: +39-91-7041041.
E-mail address: fabrizionigro@hotmail.com (F. Nigro).

0191-8141/$ - see front matter © 2004 Elsevier Ltd. All rights reserved.
doi:10.1016/j.jsg.2004.03.003

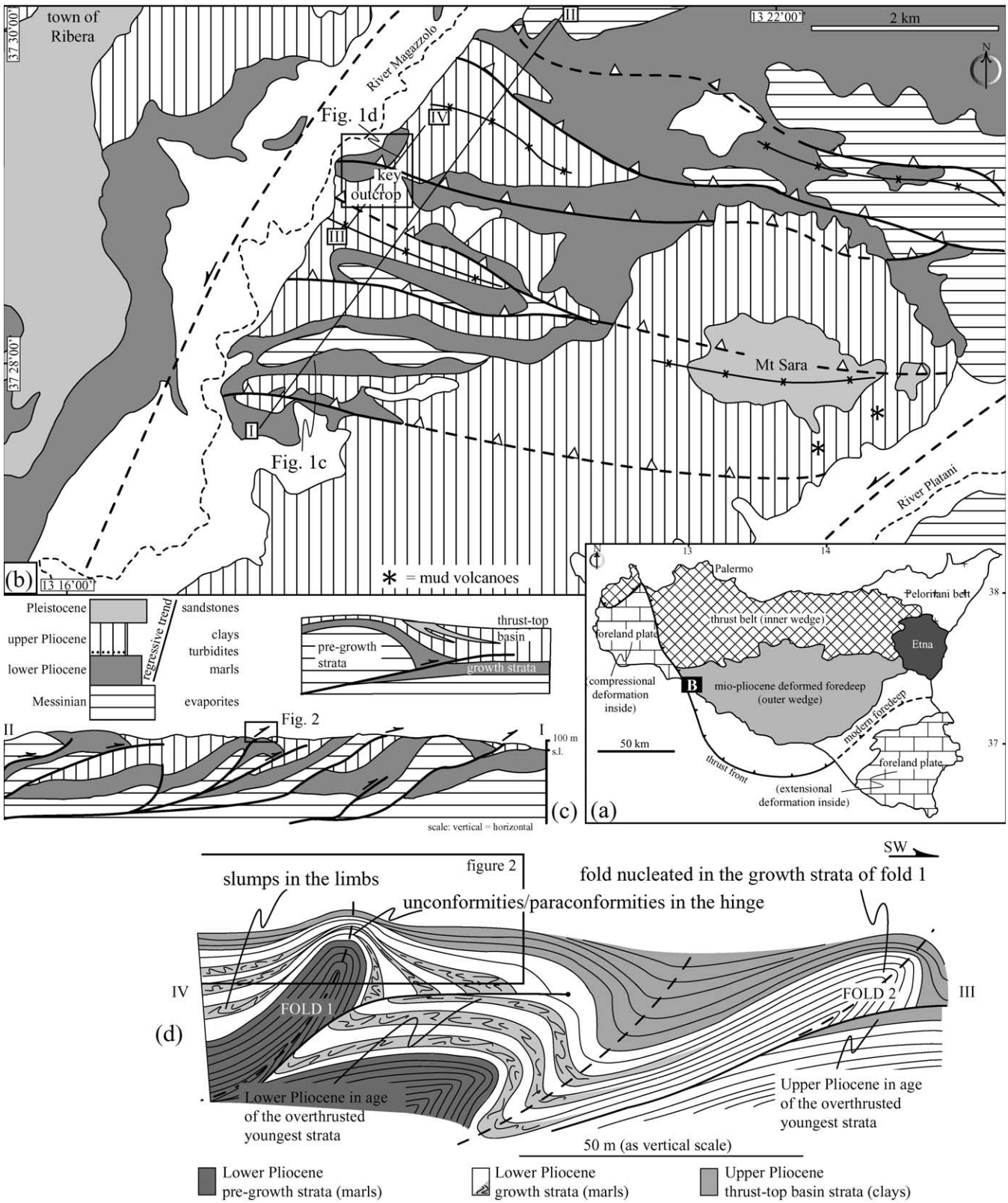

Fig. 1. (a) Tectonic sketch of Sicily. (b) Geological map and (c) cross-section of the area analysed. (d) Simplified geological section crossing the area analysed.

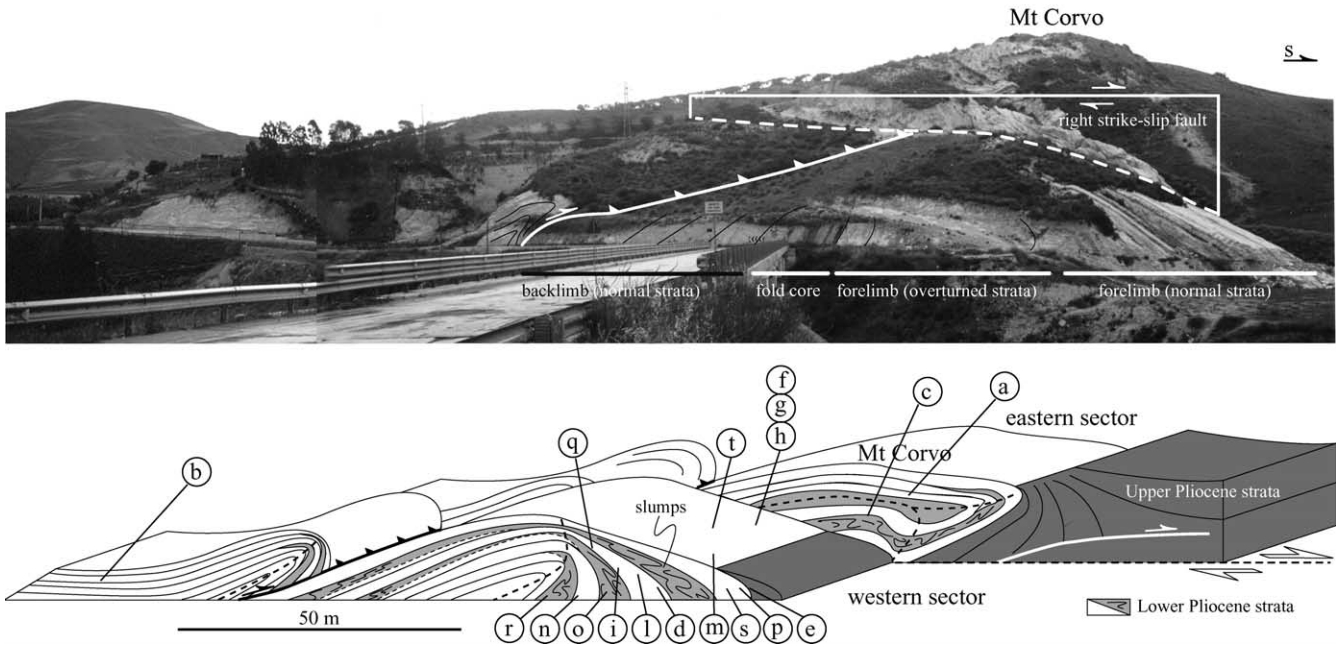

Fig. 2. Key outcrop of thrust-and-fold structures where structural analysis has been carried out. The drawing illustrates the structural setting and the circled letters are related to the photos in Figs. 3, 4 and 6.

being related to gravity-driven downslope translation or to compaction induced volume changes at all scales (Allen, 1983; Buckley and Grant, 1985; Davison, 1987; Maltman, 1994; Owen, 1995) and have been attributed to loading during slump emplacement (Shanmugam et al., 1994).

Prelithification deformation induced by tectonics has been described in convergent plate margins and is generally interpreted as the effect of sediment dewatering (Gill and Kuenen, 1958; von Huene, 1984; Bray and Karig, 1985; Carson and Berglund, 1986). Agar (1988) for example describes soft-sediment deformations and their regional relationships with folding and shearing in a contractional setting. Nevertheless, there are no detailed descriptions of field-scale relationships between folding and the response of syn-tectonic strata as regards soft-sediment structures. Also, the 'bed-by-bed' growth analysis described by Suppe et al. (1997) in deciphering the kinematic history of a well-exposed fold does not provide examples of syn-depositional minor tectonic structures within unlithified beds, which may develop under compressional deformation.

This paper aims to describe the structures affecting the poorly lithified sediments during fold nucleation and amplification in a thrust-dominated setting. The analysed field example is located in the thrust front of the Sicily Chain (Central Mediterranean), in which deformation occurred between Oligocene and Pleistocene. The syn-tectonic growth strata are composed of Lower Pliocene pelagic deposits filling the Sicily foredeep. The thrust-related fold geometries are buried by thrust-top basin deposits of Upper Pliocene–Pleistocene age. The observed stratal pattern led to the minor structures developing earlier during contractional deformation and some remarks about the geometry and kinematics of thrust-related anticlines developing within underlithified strata.

2. Geological outline

The inner chain of a southward tapering thrust belt extends W–E in Northern Sicily and is the result of the Oligo–Miocene thrust tectonics which dominated the Africa–Europe collision (Ogniben, 1960; Roure et al., 1990; Catalano et al., 2000; Fig. 1a). The tectonic units are mostly composed of Mesozoic–Lower Tertiary carbonate rocks, deposited in neritic platforms and intervening pelagic basins along the Northern Africa continental passive margin (Scandone et al., 1974; Catalano and D'Argenio, 1982).

The Upper Miocene–Pleistocene foredeep deposits crop out in Central Sicily, which were progressively involved in the compressional deformation forming the outer sector of the chain (Broquet et al., 1966; Grandjacquet and Mascle, 1978; Nigro and Renda, 2000). The foredeep strata are terrigenous turbidites and evaporites of Miocene age, and pelagic marls, clays and sandstones of Plio–Pleistocene age. The Plio–Pleistocene succession shows a regressive facies trend, from deep-water to tidal flat environments.

The tectonic wedge is thrust over the foreland plate, which crops out in Southeastern and Western Sicily. Thick

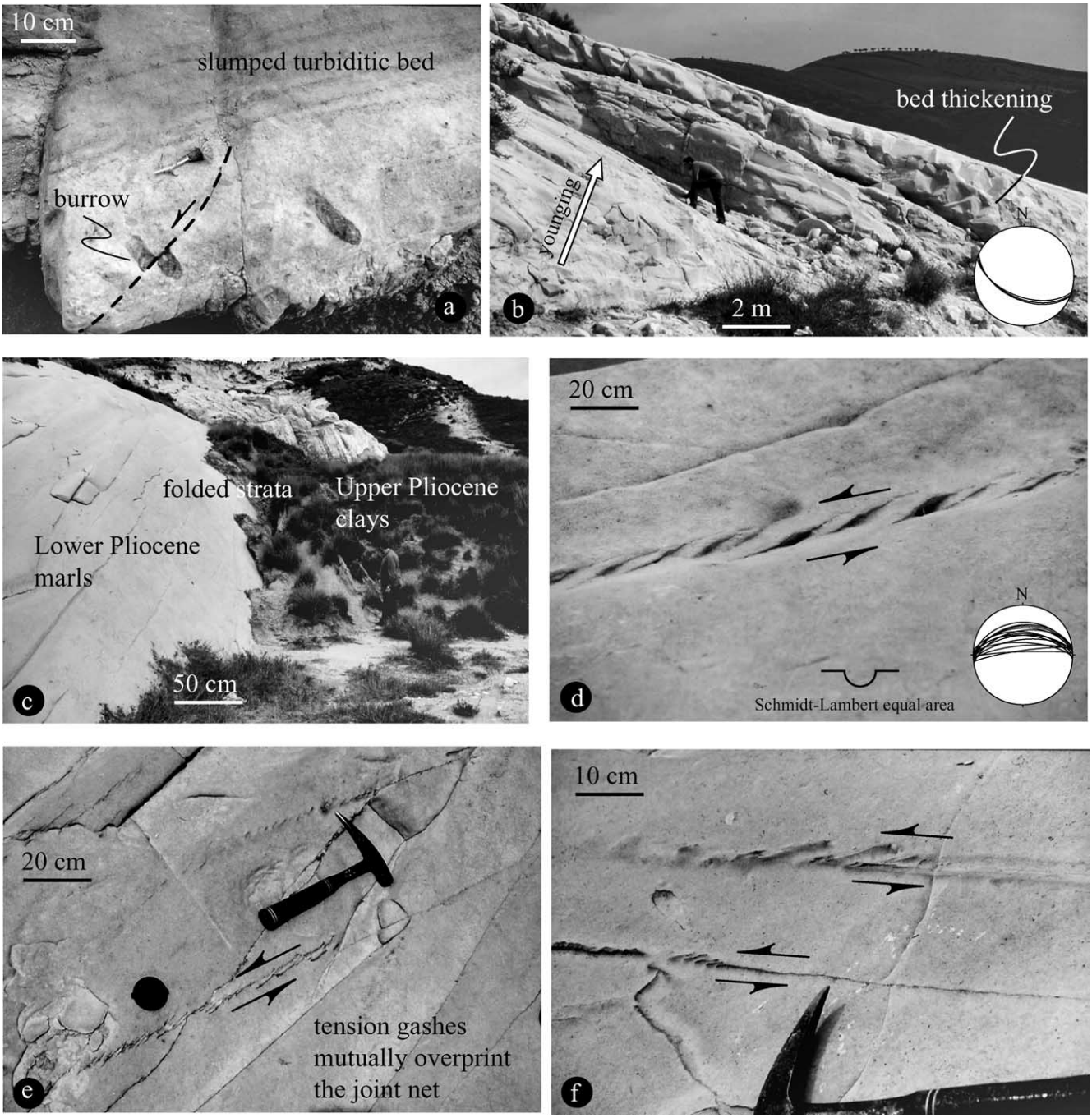

Fig. 3. Examples of structures recognised in the key outcrop of Fig. 2. Turbidites make up the forelimb (a). Normal faults easily displace the base of the graded beds, which afterwards were involved in slumps. Re-sedimentation influences the stratal geometries, which thicken downwards in the forelimb (b). Folding involved both marls and clays of Pliocene age ((e) and (c)), and occurred under a transpressional regime, as revealed by the wide presence of shear zones within the growth strata ((d)–(f)). See text for full explanation.

Fig. 4. Continued from Fig. 3. Syn-depositional small-scale normal faults (g) and boudin-like structures ((h) and (i)) widely affect the growth strata. Normal faults linked at the base of beds, are often sutured by thin horizons of marls and buried by slumped strata (l). In the forelimb the beds progressively steepen from the outer arc towards the core, where they are overturned (m). The core of the recumbent ramp anticline is affected by reverse faults that postdate folding (n). See text for full explanation.

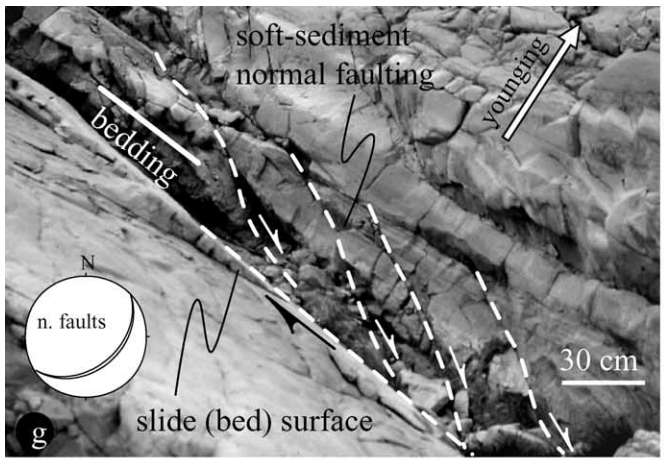

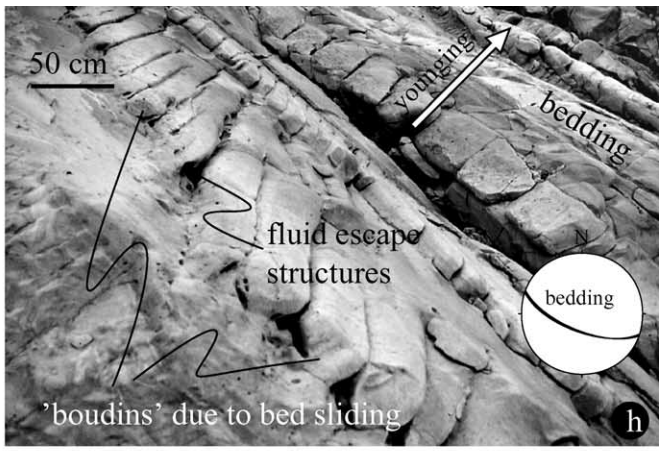

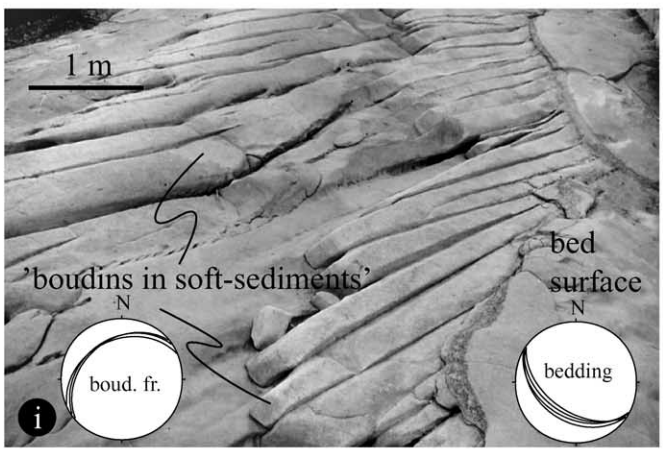

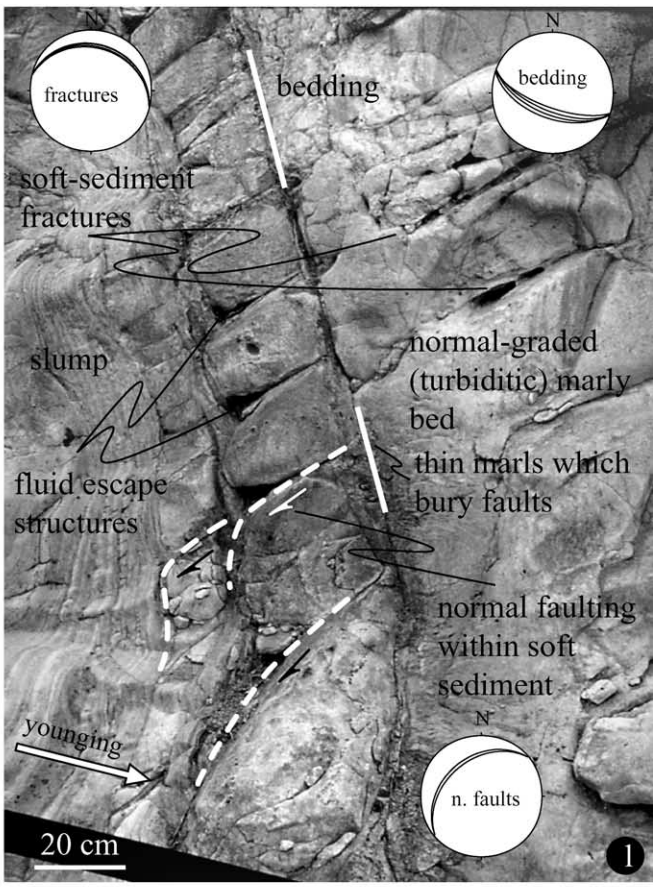

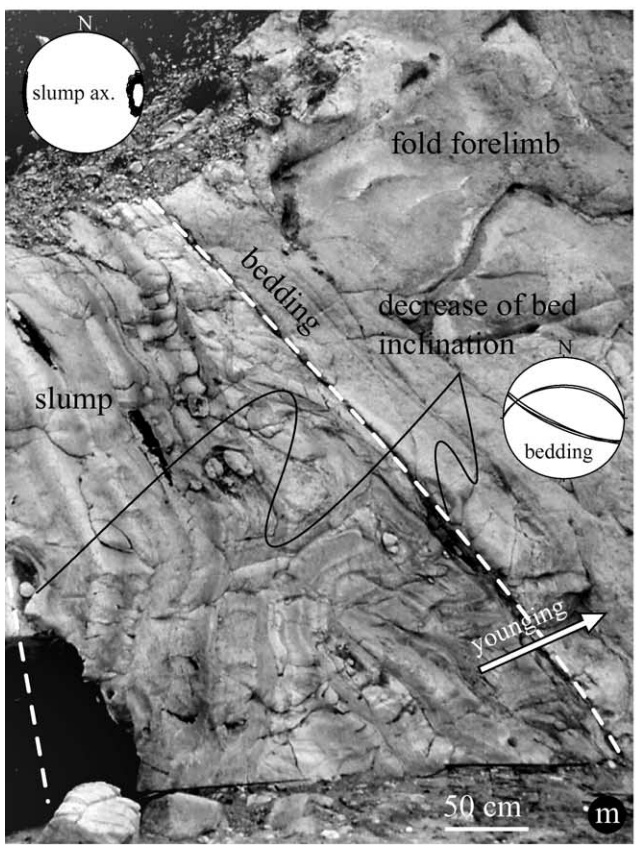

Schmidt-Lambert equal area

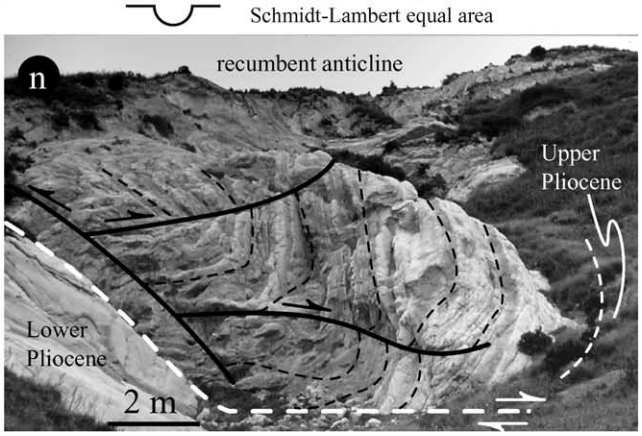

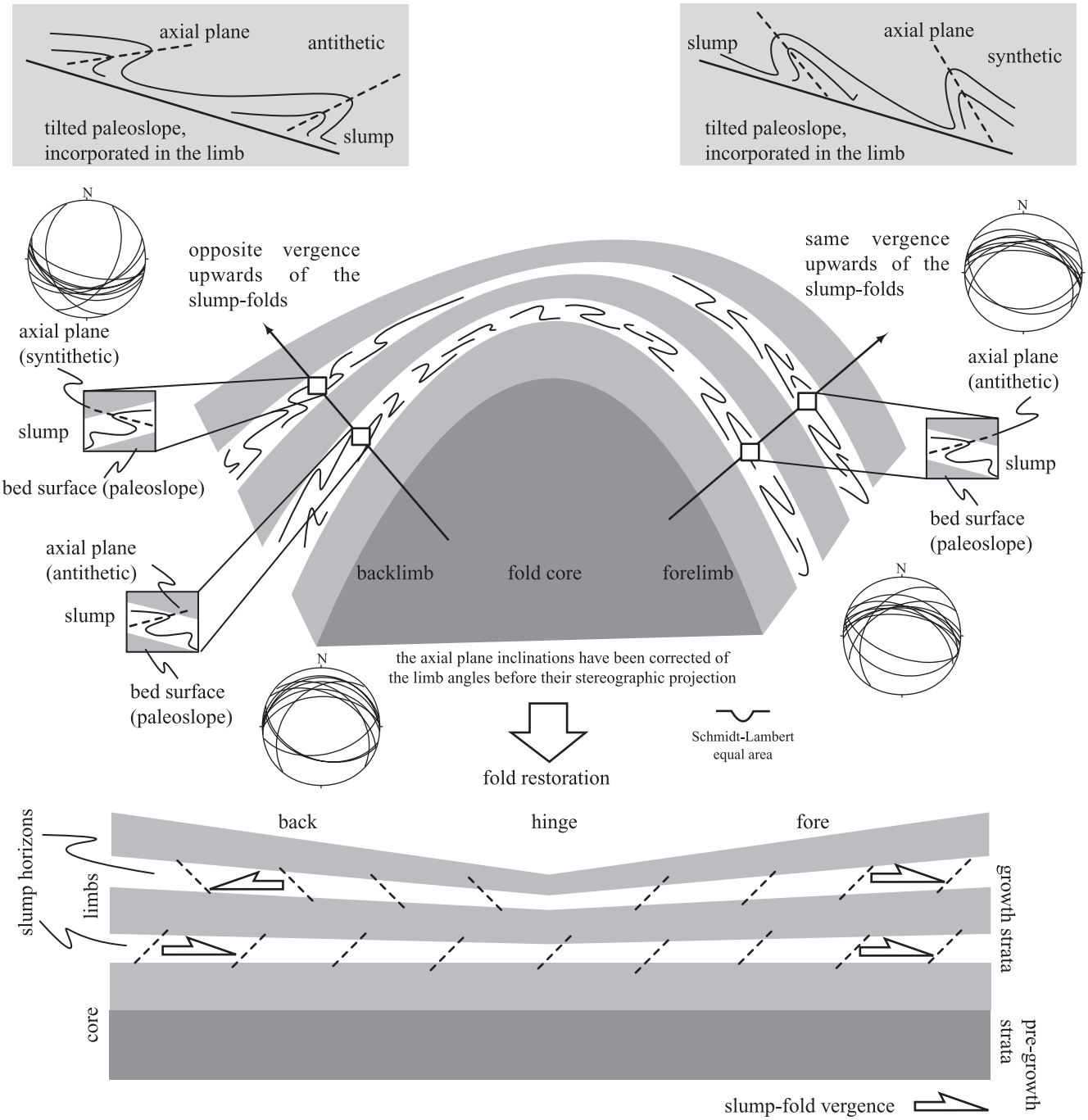

Fig. 5. Orientation of the axial planes of slump-folds sampled in the limbs of the ramp anticline. Unfolding the strata, the slump-fold vergence changes towards the younger beds forming the backlimb, as shown in the lower part of the figure.

carbonate platform strata were deposited in the foreland plate and mostly record Miocene–Pleistocene extensional deformation in Southeastern Sicily and compressional deformation in Western Sicily.

The thrust front has an arcuate geometry in map-view, which results from the influence of the indented plate boundary during the Tertiary oblique convergence (Lickorish et al., 1999).

Fig. 6. Continued from Figs. 3 and 4. In places reverse faults affect the growth strata of the forelimb (o). Locally, shear-related cleavage develops along bed separations, beyond the tip of the small-scale normal faults linkage (p). The growth strata are composed mostly of turbidites and pelagic strata, cyclically involved in slump processes (q). Differently dipping shear structures affect growth strata (r), as well as conjugate sets of bedding-normal dilatant fractures (s). See text for full explanation.

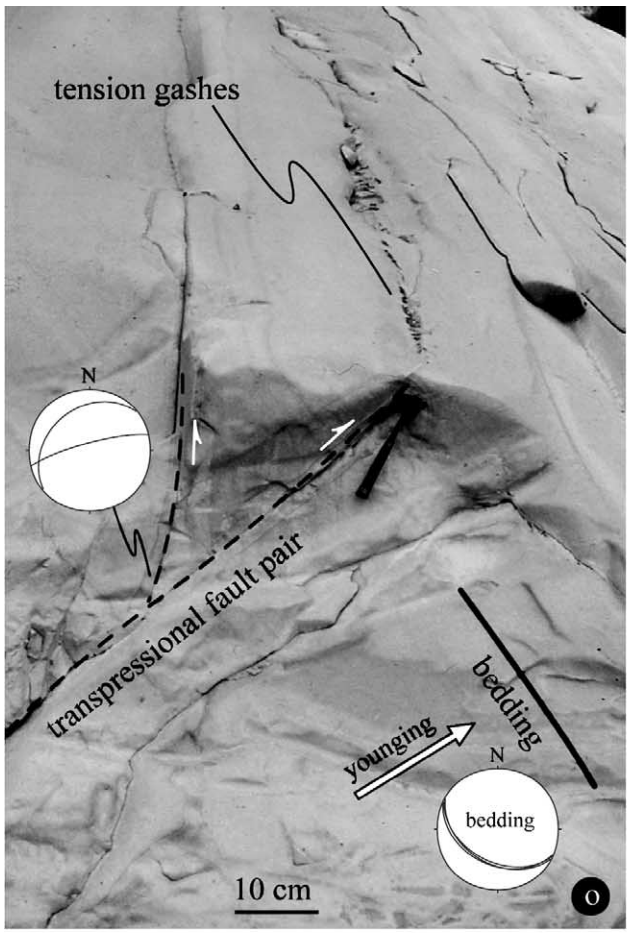

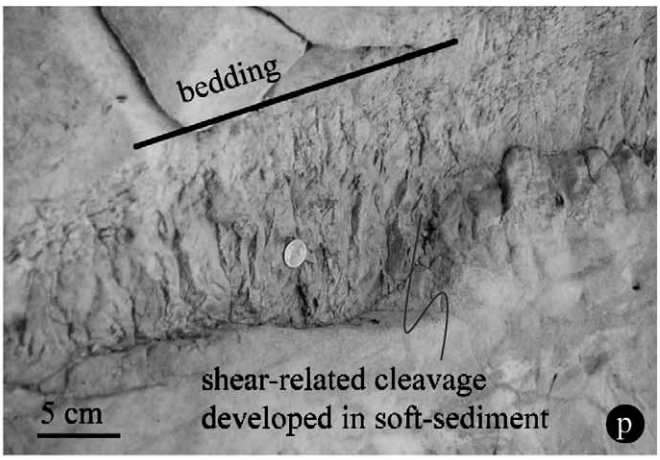

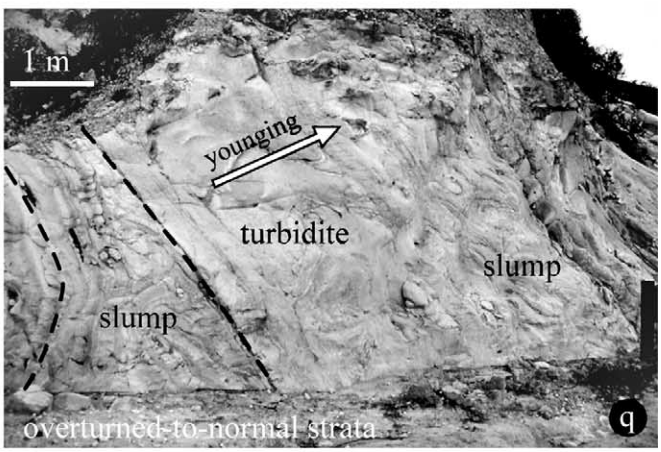

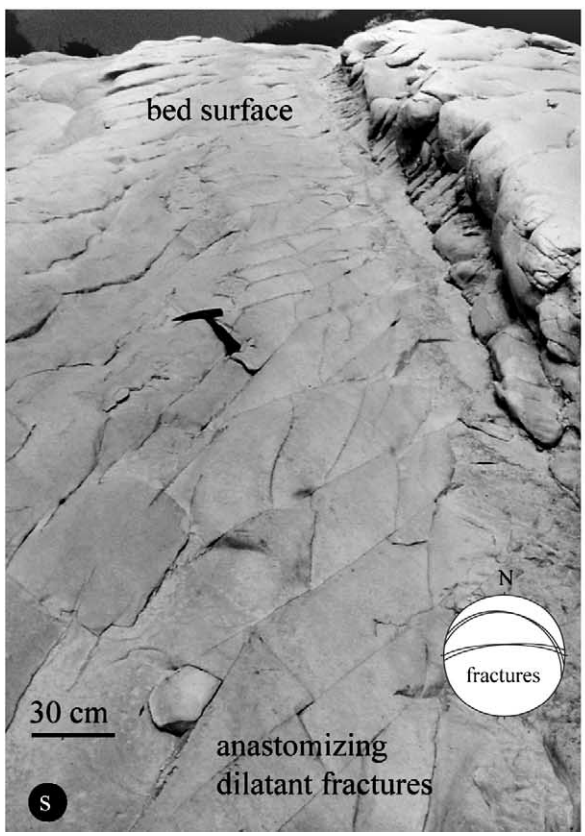

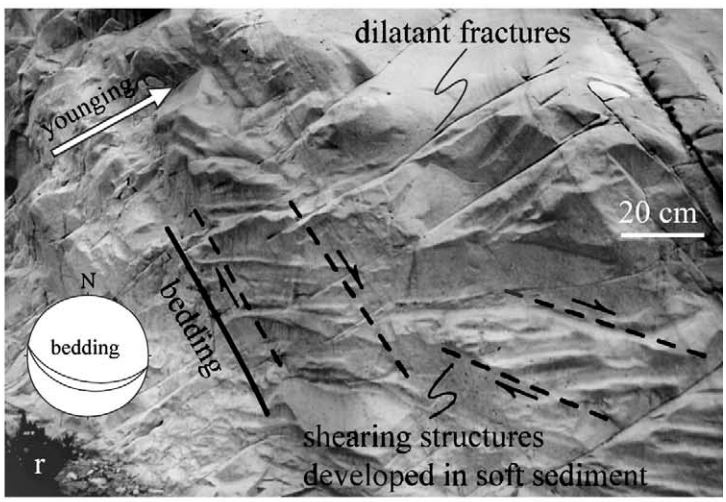

shear and dilatant fractures mutually overprint

Schmidt-Lambert equal area

2.1. Growth stratal pattern, gravity-driven and tectonic structures

In the outer zone of the chain in Southwestern Sicily, there are numerous examples where Upper Miocene–Pliocene strata display fold-and-thrust geometries within poorly lithified deposits. Thrusts and related folds are dominant structures in the region and consistently strike from W–E to WNW–ESE (Fig. 1b).

The Lower Pliocene deposits are commonly strongly folded and faulted, while the Middle–Upper Pliocene strata are increasingly less deformed. The Pliocene succession is truncated upwards by marine terraces, which are tilted and affected by southward dipping normal faults.

Thin-skinned tectonics is responsible for the deformation path recorded in the Miocene–Pliocene strata, as variously extended detachments occur within the succession, in which ramps link to form very thin sheets and duplex geometries.

The growth structures outcropping in the toe region of the Sicily chain provide useful tools in understanding the Plio–Pleistocene contractional kinematics. In the field example of Fig. 2, the Lower Pliocene deposits are affected by ductile and brittle structures. Thrust-related folds are ca. 100 m wide and the cross-section of Fig. 1d shows the fold and thrust style. From NE to SW the folds were nucleated in younger strata (Fig. 1d) and then buried by thrust-top basin fills.

The ramp anticline of Fig. 2 deforms both the Lower Pliocene white marls and the Upper Pliocene clays (Fig. 3c) and is displaced after its formation by a NE–SW-trending, dextral fault, which offsets the eastern portion of the fold southwards (Fig. 2). The western sector of the anticline is asymmetric with its axis inclined gently northwards, whereas in the eastern sectors, the fold is recumbent (see drawings of Figs. 2 and 4n). The fold axis is oriented NW–SE.

The folded strata are Lower Pliocene in age and are composed of pelagic marls, generally indicative of a low sedimentation rate. The deposits are interbedded, normally-graded marls (distal turbidites) and slump horizons, indicative of paleoslope instability. The folded strata show parallel bedding in the fold core, while the stratal pattern in the outer arc of limbs suggests a geometry that is due to growth geometries during folding. The growth strata in the forelimb dip steeply in the core and more gently towards the outer arc of fold. At the core they are overturned, dipping approximately 45°, and change progressively to upright strata dipping at approximately 50° in the opposite direction.

Within the folded strata, both gravity-driven and tectonic structures are well exposed. The gravity-driven structures were formed in soft-sediments or poorly lithified deposits, because they affect single beds or sets of beds and are overlain by younger undisturbed strata. The tectonic structures, such as cleavage and reverse faults, are well exposed in the eastern sector of the fold (Figs. 3c and 4n). In the western sector, growth strata are clearly recognisable in the fold forelimb, where the growth strata thicken down-section, forming a wedge-shaped geometry (Fig. 3b). Growth strata are characterised by gravity-driven structures, such as slumps, small-scale normal faults and intra-bed dilatant fractures (such as *boudinage*-like structures due to gravitational instabilities; Morris, 1979), formed within underlithified deposits.

Several slump horizons make up both the back- and the forelimb and are separated from each other by undisturbed, in turn fractured, beds. In the backlimb both the slumps and the bed thickening are less developed. Load-casts have been observed in the backlimb.

The thickness of the slumps is generally 1–2 m in scale and increases from the hinge downwards in the outer forearc of the anticline (Fig. 4m). Slumps decrease towards the hinge, where undisturbed pelagic beds are bounded by paraconformities. The tops of some slumps are minor irregular erosive surfaces, overlain by pelagic or graded marls (Fig. 4c). Slumps thicken more in the forelimb than in the backlimb. In the fold core, thickening is not apparent compared with the younger slump horizons in the forelimb.

Meso-scale folds in slump horizons vary in style from upright symmetrical folds and conjugate folds (less developed) to inclined asymmetrical, recumbent isoclinal and sheath folds. The upright and inclined asymmetrical folds that make up the slumps are less common in the core of the ramp anticline than in the limbs. Fold vergence within the slump horizons was sampled, in order to evaluate the paleoslope in which the unlithified strata slid, assuming that statistically the axial plane of the sedimentary folds is sub-parallel or antithetically tilted with respect to the underlying undisturbed bedding. The cartoon of Fig. 5 shows that in the fold core the axial planes of the slumps always verge southwards, whereas their vergence is southwards in the forelimb and opposite in the backlimb.

The undisturbed beds between the slump horizons are commonly affected by syn-depositional faults (Fig. 4g and l). Many faults are closely spaced, planar and connect with basal detachments that coincide with bed separations. However, some faults are apparently non-linking and can be traced into fault tips where displacement falls to zero. In places, small-scale normal faults evolve into discrete shear zones near the bed separations. Intra-bed faulting is associated with structures such as shear-related cleavage, developed locally only at the base of the faulted beds (Fig. 6p), beyond the tip of the fault linkage along the bed separation.

Extension in soft-sediments is also manifested by normal faults at the base of normal-graded beds, which displace burrows or laminations (Fig. 3a). Extensional faulting attenuates the beds in the forelimb near the fold crest. Extension near the hinge is in turn accommodated by contraction in the forelimb (Fig. 6o). Here, reverse high-angle faults deform the pelagic growth strata and diminish downwards along bed separations.

Dilatant fractures normal to bedding are formed only within the growth strata, more commonly in the graded beds. Fractures terminate at the bed separations (Fig. 4l) and affect both the undisturbed and the slumped strata. The bedding-plane exposure reveals that the fractures are anastomising (Fig. 6s) and are orientated sub-parallel to the strike of the syn-tectonic strata.

In places, fractures in the intact strata evolve into small-scale faults, which produce a tilting of blocks. In many places, these faults are overlain by slump horizons or by strata widely affected by layer-normal fracturing (Fig. 4l). The intra-bed fractures are not planar in shape and their base is more dilated than the top (Fig. 4h and l). These structures form boudin-like geometries (Fig. 4h and i) and possibly are related to fluid escape within extending strata rather than to quick loading, taking into account how they affect planar beds (see Lowe and Lo Piccolo (1974) for the description of dewatering structures without the presence of shear stress or Mills (1983) for the description of loading structures). Small-scale normal faults and fractures in turn are buried by marls a few millimetres thick, which fill the tilted blocks bounded by the discontinuities (as in Fig. 4l). On these bedding planes Nereites-like ichnofacies are very common, suggesting deep-water sedimentation.

The tectonic structures that affect the anticline are mainly represented by an axial-plane cleavage, which is well developed only in the pre-growth strata forming the fold core. Tension gashes are well developed (Fig. 3d–f). Their enveloping surfaces (Fig. 7) are sub-parallel to the strike of the beds and their inclination changes from the fold core (where they dip moderately) towards the younger beds in the forelimb (where they are sub-vertical).

Localised shear structures deform the forelimb and their enveloping surfaces rotate around the horizontal axis. Shear structures and normal-bedding dilatant fractures mutually cross-cut (Fig. 6r).

Minor folds are located in the anticline of the eastern sector and deform the already fractured beds and slumps.

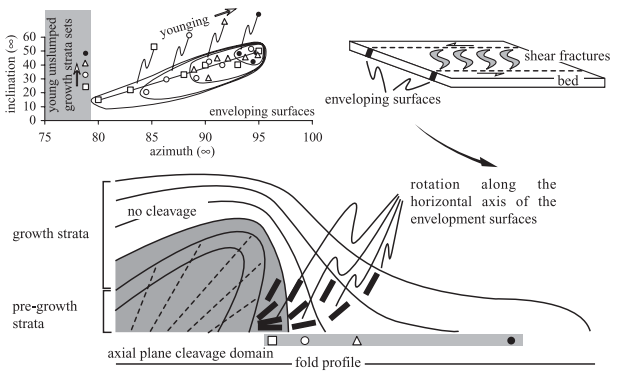

Fig. 7. Orientation of shear fractures sampled in the growth strata forming the forelimb of the ramp anticline. The graph shows that towards the core, where the axial plane lies within the pre-growth strata only, the strike and inclination of the enveloping surfaces are more dispersed than in the younger strata.

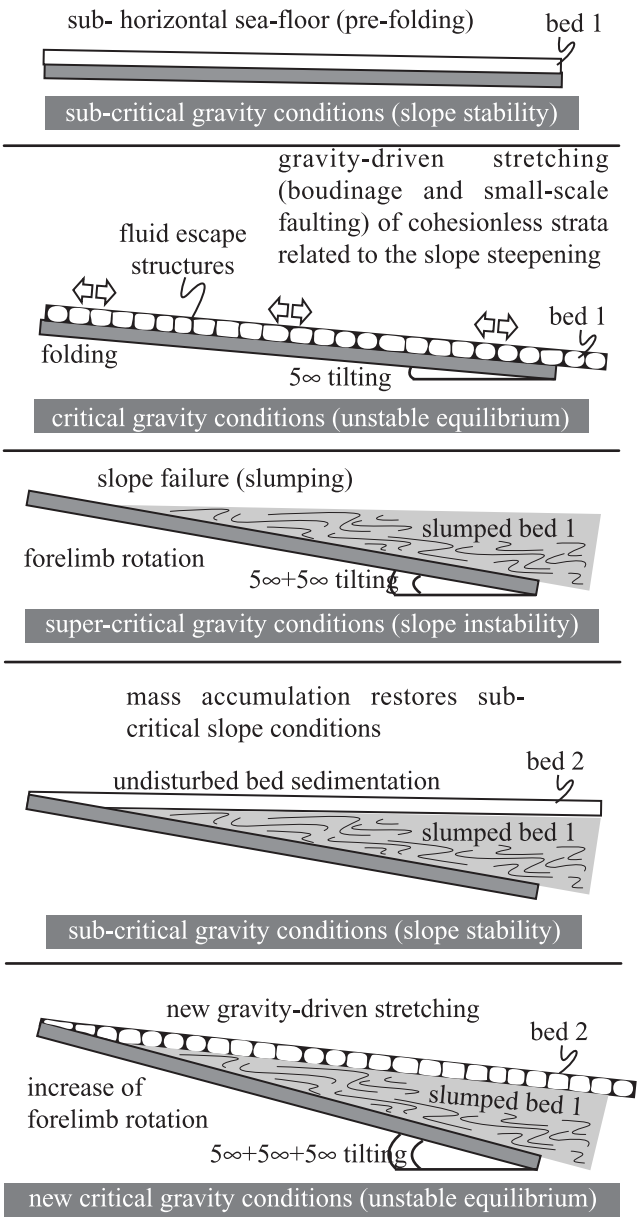

in the stratigraphic record, bed 2 may remain undisturbed, stretched or was slide to form another slump horizon, depending on the rate of lithification with respect to the rate of slope steepening (limb rotation)

Fig. 8. Time-sequence of soft-sediment structures formed during fold amplification. Fracturing occurred for low degrees of slope tilting. As the slope steepens, the gravity component parallel to the depositional surface becomes dominant and induces mass failure, demonstrated by the sliding of the beds. Slump accumulation lowers the slope inclination, allowing the deposition of new undisturbed beds, in which fracturing occurs for further slope tilting. Lithification of the slump mass inhibits the propagation of fractures downwards.

The fold core is affected by reverse faults (Fig. 4n), which displace the minor folds. In the damaged zones containing the reverse fault planes (less than 1 m wide), cleavage is present, which overprints all the gravity-driven structures described within the growth strata.

3. Interaction between gravity-driven mass failure and thrust-fold kinematics

The structures analysed, which developed in underlithified syn-tectonic deposits in Sicily, indicate that there is a great contribution by the sedimentary processes coeval with contractional deformation to the final fold geometry, due to soft mass re-distribution over the mobile slope. The sediments undergo changes in equilibrium related to the slope steepening during limb rotation. Stretching or re-sedimentation processes in active slopes may develop if the shortening rate in thrust-dominated tectonics, in terms of limb widening/steepening, is higher than the process of lithification that affects syn-tectonic deposits.

The stability of underlithified, cohesionless sediments also depends on the angle of slope, ignoring pore fluid pressure, seismic impulse, etc. The inclined mobile surfaces, such as thrust-related fold limbs, may steepen during fold amplification higher than the angle of internal friction of the syn-tectonic deposits. Mass re-distribution takes place from the hinge towards the base of limbs.

Syn-tectonic strata may be subjected to failure during the process of lithification, depending on the 'burial compaction/limb tilting' ratio (Fig. 13).

We suggest that the soft-sediment structures in question were formed by gravity failure resulting from the tectonically-induced slope tilting: the gravity acted in both soft-beds (turbiditic horizons) and poorly lithified sets of beds (slumps).

The syn-faulting thin horizons in which ichnofacies develop, burying the stretched beds, suggest that fracturing occurred within unconsolidated beds near the surface, where burial pressure coincides with hydrostatic pressure. As generally indicated by the geometric features of the fractures crossing the folded strata, the regularly spaced bedding-normal dilatant fractures and the boudin-like structures indicate moderate layer-parallel stretching developed before the slumps, taking into account how they are contained in the folded beds within the slid horizons. Their occurrence resulted from a few degrees of tilting (Fig. 8) and dilation of walls was easily increased by upward fluid flows. Increases in tilting higher than the angle of internal friction of sediment induced failure and the mass-accumulation downwards reduced slope inclination, restoring sub-critical slope conditions (Fig. 8).

During continuing sedimentation on a less steep slope, in which mass-movements are inhibited, new bed fracturing may develop as a consequence of the further tilting of the substrate. New fracturing does not cross down into the slump substrate, because of its lithification difference with respect to the soft young bed. Limb rotation during fold amplification leads to repeated slope failure; the rhythmic sedimentary pattern derives from the gravity-driven bed-by-bed deformation, such as bed stretching and slumps, in poorly lithified media.

Fold uplift controlled the distribution of the slump bodies. The common presence of upright symmetrical folds and inclined asymmetrical folds developed into slumps which are incorporated in the outer arc of the ramp anticline implies that the material has been translated short distances (as described by Farrell and Eaton (1988)). The wide presence of recumbent folds in slumps forming the core of the ramp anticline implies long-distance down-slope translation during simple-shear longitudinal shortening of the slump (Farrell and Eaton, 1987).

The statistical orientation of the axial planes of slump folds, and their inclination, also indicates that vergence is constant in the strata which form the forelimb, but changes progressively with age of strata in the backlimb (Fig. 5). This change of vergence reflects the change of slope inclination and subsequently of the source area of the failed mass. Fold nucleation in the slope where slumps already occur may result in the slope itself becoming a new source area for the sliding of unstable soft bodies during folding-induced uplift.

Slumping restores slope stability following limb tilting and cyclically allows sedimentation in a less tapered depositional surface. Fig. 9a shows the difference between surface slopes formed during progressive limb tilting with and without accompanying slope failure and slumping (Fig. 9b).

Many tectonic structures and their overprinting relationships indicate that they also occurred during limb tilting, as

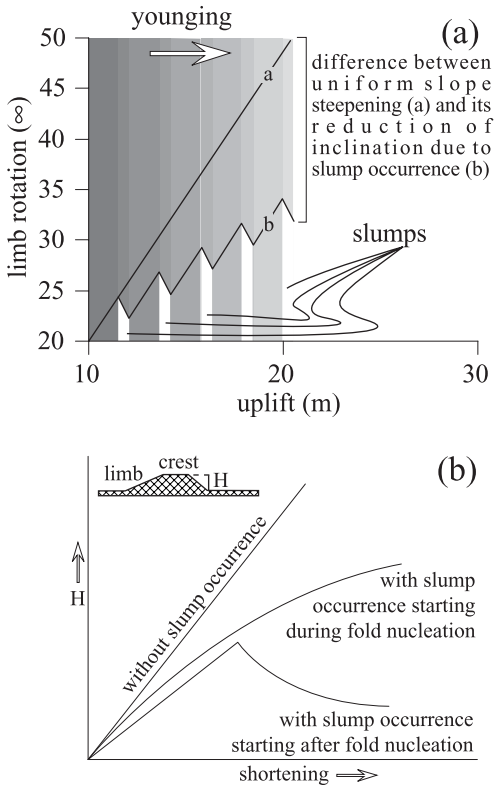

Fig. 9. Slump occurrence progressively reduces the dip of the forelimb during fold amplification and uplift (a), reducing the height between the fold crest and the base of limbs (b).

the geometric relationships between bedding and the earlier tectonic structures developed within the underlithified sediments. For example, within the forelimb, the strike and inclination of the gash veins (Fig. 3d–f) is more dispersed in the older strata than in the younger (Fig. 7). The change in strike implies rotation along the vertical axis during folding, in addition to the change of inclination in the direction of younging, which indicates forelimb rotation. The shearing structures (data of Fig. 6r) formed before complete lithification, as suggested by their mutually overprinting relationships with the dilatant fractures.

Evidence of limb rotation during the early stage of lithification is also supported by the change of inclination of these shear fractures. The progressive tilting of the growth strata has as a consequence the clockwise rotation of the older shear fractures, with the progressive overprinting of new, less inclined, shear sets. The difference of inclination reflects the amount of limb rotation during the growth bed deposition in which the shear structures developed.

The growth bed geometry acquired during thrust-related folding is shown in Fig. 10. The fan geometry of growth strata in the forelimb derives mainly from bed thickening, as a result of slump mass accumulation. The inclination of the overturned pre-growth strata in the fold core suggests about 135° of limb rotation during folding.

Thrust propagation folding formed through layer-parallel shear, thus allowing fold asymmetry. Fold amplification developed with progressive axial plane inclination, resulting in fold asymmetry and in turn recumbent geometry. Asymmetric fold development under simple shear conditions resulted from passive rotation of folds during increasing shear strain. The simple shear strain in the thrust hanging-walls may result in a reduction of the rate of displacement near the base of the asymmetric ramp anticlines, and enables the identification of recumbent thrust-related folds.

Tectonic structures, such as high-angle reverse faults and related cleavage affecting the core of the ramp anticline, occurred later than the lithification processes and overprint soft-sediment structures. Fig. 11 depicts the development sequence of the structures that affected soft-sediment during thrust-related fold nucleation and amplification, characterised by a continuous change of forelimb geometry. Fig. 12 shows the kinematic evolution, characterised by the rhythmic restoration of sub-critical conditions for sediment accumulation in the unstable forelimb. The reverse faults affecting the core of the recumbent ramp anticline indicate a later rupture during fold amplification. Thrust migration develops forelandwards through fold nucleation within younger strata (Fig. 1d).

Thrust geometries are generally reduced to two-dimensional geometric models (fault-bend folding of Suppe (1983); fault-propagation folding of Suppe and Medwedeff (1984, 1990)). They are used in a forward modelling sense to predict hanging wall geometries (e.g. Mitra, 1990; Mosar and Suppe, 1992; Suppe et al., 1992; Zoetemeijer et al., 1992).

The modes of sedimentation during fault slip and associated fold growth (growth strata) have been accurately described by Mount et al. (1990) and Suppe et al. (1992). But these models don't adequately take into account mass conservation (because they treat erosion as the instantaneous loss of pre-growth strata above a given base level) and assume that sedimentation is independent of deformation. Also, the base level is usually defined as a dimensionless ratio of sedimentation rate to ramp uplift.

Hardy and Poblet (1995), using the general tectono-sedimentary forward modelling equation of Waltham (1992), present two-dimensional mass-balanced numerical models of fault-bend and fault-propagation folding, which include the effect of erosion, transport and sedimentation, allowing bathymetry or structural relief to develop in the region of a growing fold. The tectono-sedimentary forward modelling equation of Waltham (1992) combines sedimentary and tectonic processes as:

$$\partial h/\partial t = [p - \partial F/\partial x] + [\nu - u\partial h/\partial x]$$

where h is the height of a surface at a fixed horizontal location, t is time, p is a source term, F is the sediment flux, x is a horizontal coordinate, ν is the vertical velocity (uplift or subsidence) and u is the horizontal velocity. The first term for right of the sign of equality expresses the sedimentary processes, while the second expresses the tectonic processes. This equation combines sedimentary and tectonic processes starting from the concept that the height of a geological surface can be modified from: (a) the material which can be added to or subtracted from the surface or (b) can be moved from one part of the surface to another; (c) the surface can be physically moved or (d) deformed.

The growth strata geometries which form during the translation of the fault-bend and fault-propagation folding processes described by Hardy and Poblet (1995) derive from velocity models, with the addition of sediment erosion, transport and deposition. The relationships between the time of sediment compaction and the vertical velocity are not considered by Hardy and Poblet (1995), nor are several of the rock properties (the porosity, the cohesion, the angle of internal friction) of the syn-tectonic strata. The equation of Waltham (1992) does not consider the kind of material that was deposited during thrusting and folding. The porosity, cohesion and angle of internal friction are characteristics of the sediments and their time-variance (porosity decreases and cohesion/angle of internal friction increase) depend on the sediment compaction and lithification rates. These physical properties influence the term of the Waltham's equation, which describes the tectonic processes. The height of surface h and the vertical velocity ν develop in different ways; for example, during sedimentation of clays or coarse-clastics or calcareous muds. The relationships between the uplift rate (and the related limb tilting of a thrust-related fold) and the physical properties of the materials or their rate

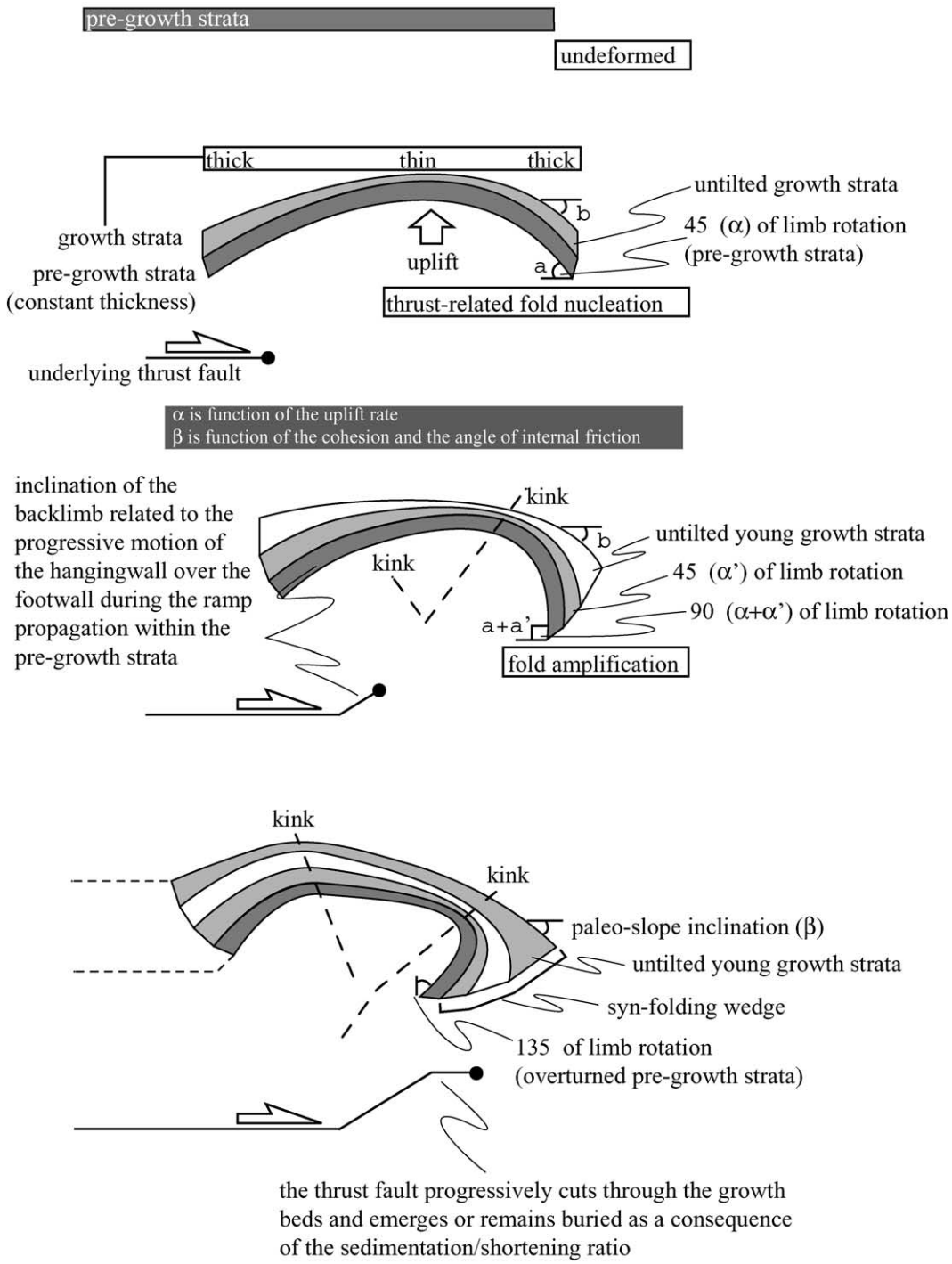

Fig. 10. The forelimb wedge geometry of the ramp anticline may be described in terms of the progressive tilting of beds, which occurs simultaneously with slope flattening as a consequence of slump occurrence. Slope instability is strictly related to the limb-hinge kinematics, as an expression of the underlying thrust fault propagation.

of lithification change the fold-growth geometry. Hence, Waltham's equation may assume the following form:

$$\partial h/\partial t = [p - \partial F/\partial x] + [\nu - u * \partial h/\partial x] + P$$

where P represents the physical properties of the material (cohesion and angle of internal friction) and the process of lithification (time of sediment hardening, depending on the porosity reduction, the chemical processes due to the interstitial fluid circulation, etc.).

As well as the tectonic structures, gravity-driven structures are formed within underlithified strata due to the paleoslope instability deriving from thrust-fold nucleation. The progressive steepening of the slope may be attributed to limb rotation during fold amplification and is

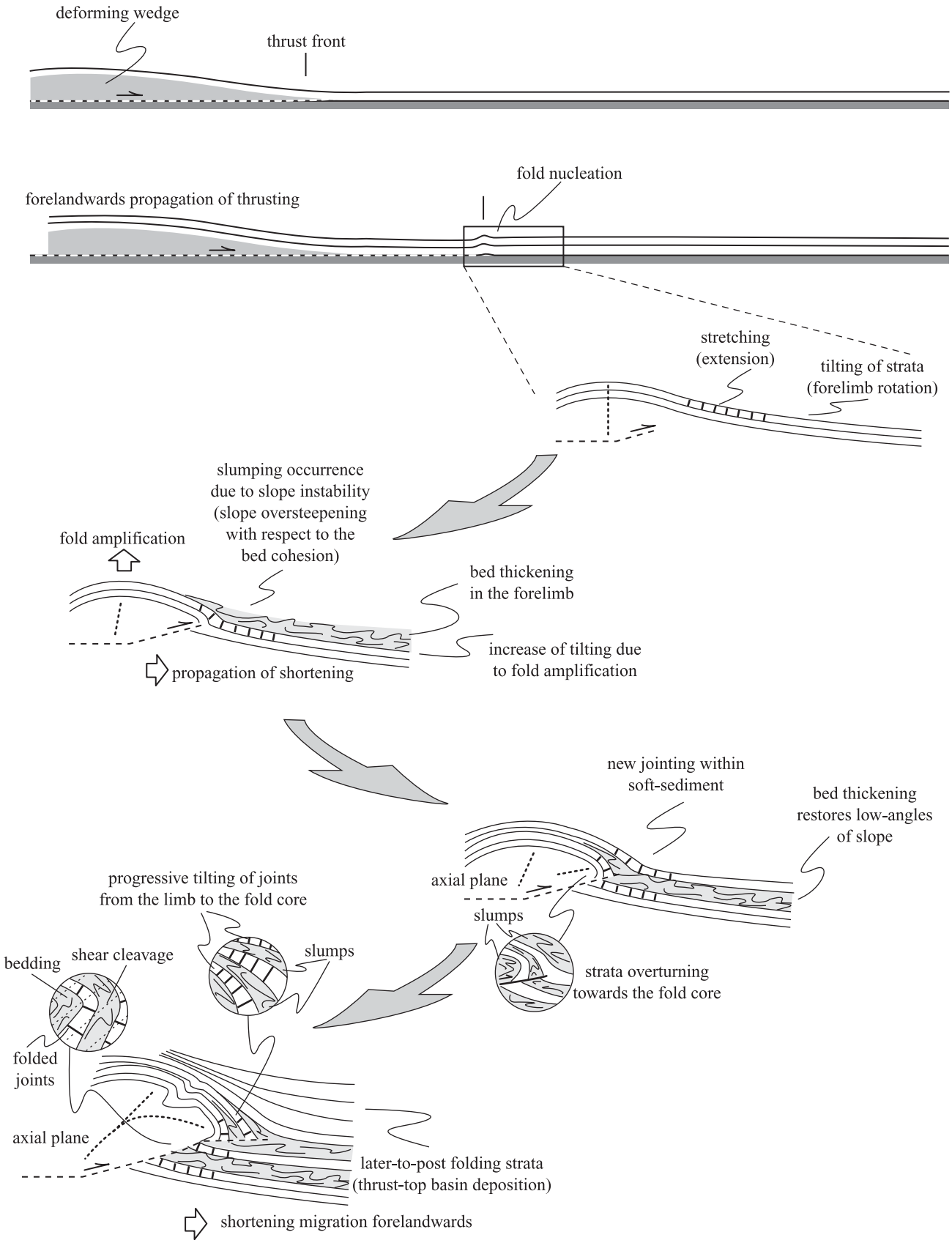

Fig. 11. Sequence of development of gravity-driven soft-sediment structures in the fold growth strata, later affected by tectonic structures, as the underlying thrust fault propagates forelandwards.

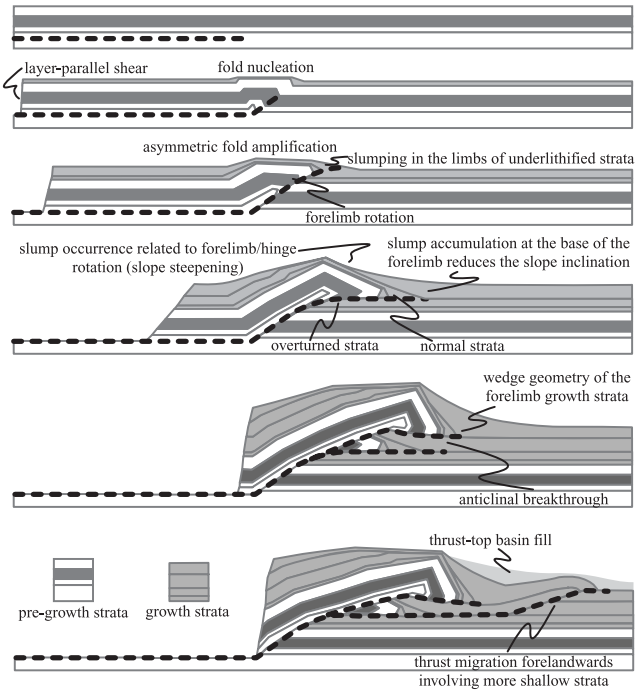

Fig. 12. Kinematic evolution characterised by thrust-related asymmetric fold amplification within underlithified deposits. Forelimb rotation acts as an instability mechanism for syn-tectonic sediments, which rhythmically slide and accumulate at the base of the limb, lowering slope tilt. Anticlinal breakthrough took place later and the associated high-angle reverse faults and cleavage overprint of the structures occurred in the underlithified fold-growth strata.

recorded in the growth pattern of the foreland thickening strata-set incorporated into the anticline. The mobile depositional surface acts as a driving mechanism for the development of the observed soft-sediment structures, such as boudinage, intra-bed fractures and slumps.

When the slope steepens, the equilibrium of soft-sediment changes towards instability. As predicted by the Coulomb–Mohr equation, for sediments deposited upon an inclined surface, such as a slope in which lithification is not or not completely developed, and which is undergoing hydrostatic loading only, its stability is related to many properties such as grain-size and chemical composition, cohesion (c) and the angle of internal friction (ϕ).

The critical shear stress at failure τ can be related to the angle of internal friction ϕ and cohesion c by the expression:

$$\tau = c - \sigma' \tan\phi \tag{1}$$

where σ' (effective pressure) is equal to $\sigma - u$ (σ is total normal pressure and u the pore pressure). For granular sediments, even if composed of fine grain-size particles (such as the marls outcropping in the analysed area), cohesion may be disregarded before the onset of their lithification due to their unpacked nature and high water content.

In the finer sand grades, the grains are more subject to loose metastable packing, negligible cohesion and low permeability, thus allowing for maximum application of deforming shear stresses.

The expression (1) may be rewritten as:

$$(\rho_s g z \cos\alpha)\sin\alpha = (\rho_s g z \cos^2\alpha - \rho_w h g \cos^2\alpha)\tan\phi \tag{2}$$

where: ρ_s = wet sediment density; ρ_w = water density; g = acceleration due to gravity; z = altitude of the depositional surface (with respect to the sea level; positive if subaerial, negative if submarine); h = water level (equal to z if submarine); α = slope inclination; if $w = h/z$ (equal to one for submarine conditions), then, for failure:

$$w = \rho_s/\rho_w(1 - \tan\alpha/\tan\phi) \tag{3}$$

but, for $w = 1$

$$\tan\alpha = (1 - \rho_w/\rho_s)\tan\phi$$

and then

$$\alpha = \arctan[(1 - \rho_w/\rho_s)\tan\phi] \tag{4}$$

The sediment failure along an inclined depositional surface (slope) may take place from zero, when $\alpha = \phi$ to a maximum of ρ_w/ρ_s, when $\tan\alpha = 0$ (flat surface). If $\tan\alpha < (1 - \rho_w/\rho_s)\tan\phi$, the sediment is always stable, whereas if $\tan\alpha > \tan\phi$ the sediment is always unstable.

For submarine deep-water environments generally dominated by low-energy tractive currents, the slope inclination (α) is the main influence on the equilibrium of the sediments: if $\alpha > \phi$, the deposits become unstable and slump processes take place. Gravity-driven sediment instability decreases inversely with the lithification process and can be discussed in terms of porosity reduction for burial compaction, as argued by Schlanger and Douglas (1974) and Schmoker and Halley (1982 and references therein) for limestones of different ages.

The above described relationships between the physical properties of the sediment and the inclination of the depositional surface may be discussed in terms of kinematic constraints. In the fault-bend folding model, the dip of the fault (θ), the axial angle of the fold (γ) and the dip of the forelimb (β) are related by the following equations:

$$\tan\theta = \sin^2\gamma/(2\cos^2\gamma + 1)$$

$$\beta = 180^\circ - 2\gamma \tag{5}$$

These equations hold only for fault dips $<30^\circ$ (Suppe, 1983).

In the fault-propagation folding model, Suppe and Medwedeff (1990) derived a series of equations defining angular relationships for the fixed-axial surface theory. For a simple step, fixed-axis fault-propagation fold, the fold interlimb half angles (γ_i, γ_1^*, γ_e, γ_e^*) are related to the footwall cut off angle (θ) and shear (S_p) by the following equations (see fig. 1 in Hardy and Poblet, 1995):

$$\gamma_i = \sin^{-1}[\sin\gamma_i^* \sin\gamma_e)/\sin\gamma_e^*]$$

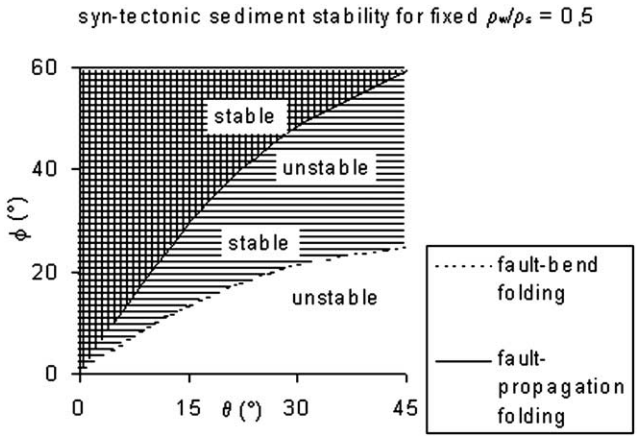

Fig. 13. The graph shows the relationships between ϕ and θ in both (fault-bend and fault-propagation) folding models. In the left sectors bounded by the two curves, the syn-tectonic sediments are stable for fixed density ratio ρ_w/ρ_s. Vice versa, in the right sectors failure occur (slumping), as a consequence of the exceeded values of the thrust fault inclination θ (and in consequence of the forelimb inclination) with respect to the angle of internal friction ϕ. The range of sediment stability in the fault-bend folding model is represented by the area marked by the horizontal lines pattern; the range in the fault-propagation folding model is marked by the vertical lines pattern. θ ranges from 0 to 45°, ϕ from 0 to 60°.

$$\gamma_e = \cot^{-1}[\cot\gamma_e^* - 2\cot\gamma_1 - S_p]$$

$$S_p = 2\cot\gamma_e^* + (2\cos\theta - 3)/\sin\theta$$

$$\gamma_1 = \gamma_i^* + \gamma_e^*$$

$$\theta = 180° - 2\gamma_1$$

the dip of the forelimb is (Suppe and Medwedeff, 1990, eq. 26):

$$\delta = \gamma_1 \quad (6)$$

The slope inclination α coincides with β in the fault-bend folding and with δ in the fault-propagation folding model. So, in terms of sediment failure during fold nucleation and amplification, Eqs. (5) and (6) may be rewritten as:

$$(\text{fault} - \text{bend folding})\ \tan\theta = \sin^2(90° - \alpha/2)/[2\cos^2(90° - \alpha/2) + 1] \quad (7)$$

$$(\text{fault} - \text{propagation folding})\ \theta = 180° - 2\alpha \quad (8)$$

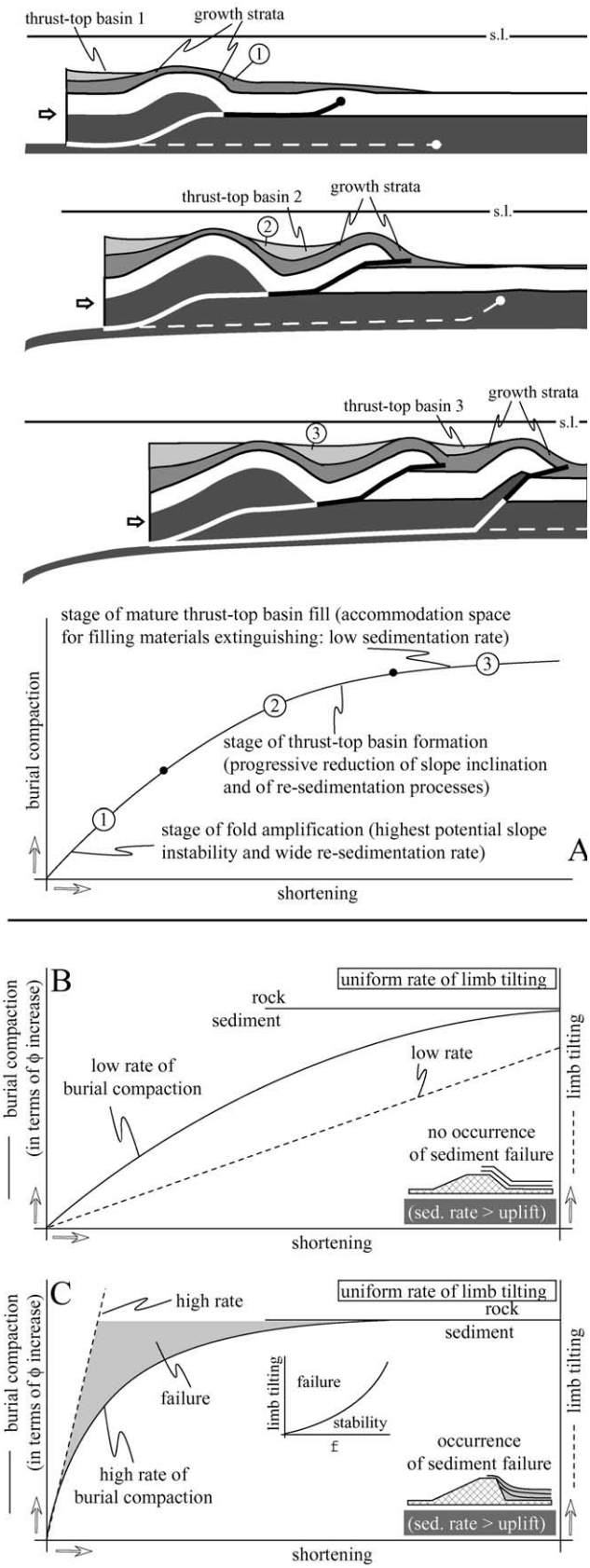

Fig. 14. (a) Qualitative graph showing the change of burial compaction during thrust-related basin formation (compared with the three stages of the kinematic evolution upwards), in terms of sediment supply or resedimentation occurrence along the mobile steepening slopes (fold limbs). Qualitative graphs showing that the occurrence of sediment failure in the fold forelimb is a function of the lithification/slope steepening ratio. (b) If the ratio is high than one, no sediment failure occurs. (c) For ratio less than one, the sediment is subjected to instability. See text for full explanation.

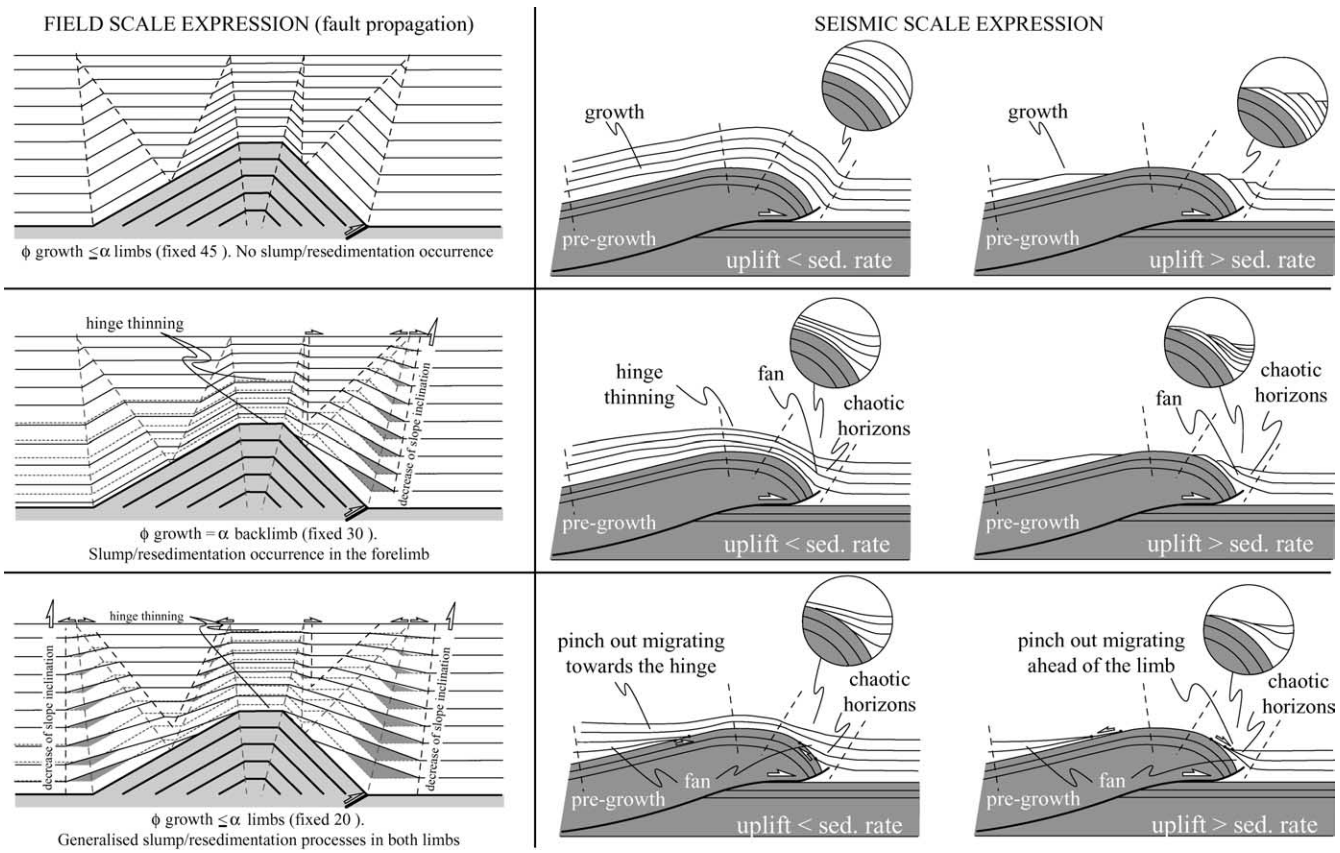

Fig. 15. Field expression (left side) and seismic expression (right side) of the change in thrust-related fold geometry. Growth strata, until their lithification, continuously determine slope inclination (α). The physical properties of the underlithified sediments, such as the angle of internal friction (ϕ), deposited on the mobile slope, fix the conditions of mass stability. The relationships between α and ϕ can be set forth in terms of the limb rotation rate (and then uplift) versus lithification. In the case of sediments in which lithification develops earlier (such as carbonates and marls), if the amount of limb rotation is greater than the lithification rate, mass re-sedimentation repeatedly takes place in the limb steepening more than the value in ϕ of the sedimented bed. The thickness of growth strata near the fold hinge is a linear function of ϕ. When there are low values of ϕ the hinge may not be buried by the growth strata, even if the sedimentation rate is higher than the uplift rate. This geometry may be amplified for deposits in which lithification develops slowly. Low values of ϕ determine the wedge geometries of limbs and pinch-out stratal terminations. At the seismic-scale the pinch-out geometries may migrate towards or beyond the hinge as a consequence of the uplift being dominant or not with respect to the sedimentation rate.

and, for Eq. (4):

$$\tan\theta = \sin^2\{90^\circ - [\arctan(1 - \rho_w/\rho_s)\tan\phi/2]\}/\{2\cos^2[90^\circ - \arctan(1 - \rho_w/\rho_s)\tan\phi/2] + 1\} \quad (9)$$

$$\theta = 180^\circ - 2[\arctan(1 - \rho_w/\rho_s)\tan\phi] \quad (10)$$

Eq. (9) relates to the fault-bend folding model, whereas Eq. (10) relates to the fault-propagation folding model. Eqs. (9) and (10) relate the thrust step-up angles to the physical properties of the syn-tectonic sediments which form the growth strata in the fold forelimb of the ramp anticlines. The equilibrium of soft-sediments depends on the inclination of the thrust ramp and, for a fixed step-up angle, on the density and the angle of internal friction. Fig. 13 shows, for both folding models, the range of stability of the syn-tectonic sediments with respect to the thrust fault inclination. The sediment failure is related to the spatial development of the thrust ramp and its propagation rate (which must be higher with respect to the compaction/lithification rates of the growth deposits to induce slumping phenomena).

The sediment supply during thrust-related folding changes with shortening propagation, related to mass failure, and subsequently to the rate of burial compaction cut sites of sediment accumulation (i.e. at the base of fold limbs; Fig. 14a). If the limb tilting is uniform over time and less than the sediment 'hardening', fold amplification develops without mass failure (Fig. 14b). Vice versa, a high rate of limb tilting induces sediment failure, even under a high rate of burial compaction (Fig. 14c), which, for example, occurs in the forelimb as a consequence of extensive resedimentation processes.

Considering the interaction between the inclination of the depositional surface and the physical characteristics of the poorly consolidated, cohesionless sediments, such as the angle of internal friction, the growth geometries of Fig. 15 are different to the predicted patterns (Suppe et al., 1992; Storti and Poblet, 1997) for thrust-propagation folding

(Suppe and Medwedeff, 1990). For ϕ higher than the limb inclination (fold amplification lower than lithification rate) the growth pattern is the same as the current models (Suppe et al., 1992). If ϕ decreases (or the fold amplifies faster than the lithification rate of the syn-tectonic strata), fan geometry develops in the steepening limb and the fold hinge quickly attenuates. The inclined portions of growth strata are wider than predicted in the pattern of Suppe et al. (1992). For low angles of internal friction, growth strata undergo a lessening of inclination in the limbs and in the early stages of fold amplification and uplift they may not bury the pre-growth folded strata, even if the sedimentation rate is higher than the uplift rate.

The seismic expression is shown in the right part of Fig. 15. Progressive decrease of ϕ determines seismic-scale growth fan and the pinch-out stratal pattern in the fold limbs. Pinched stratal terminations may migrate towards or beyond the hinge, depending on the uplift rate being less or higher than the sedimentation rate, respectively.

The growth geometries of Fig. 15 are similar with those of the models of Hardy and Poblet (1995); the differences relate to the contribution of the syn-tectonic sediments (in particular of their physical properties) to the wedge-drape stability with respect to the mobile substrate. Our conclusions are that in both forelimb and backlimb growth strata, a further thickening may occur beyond that in the models of Hardy and Poblet (1995), depending on the amount of slope tilting (fold amplification), rate of shortening (ramp-flat propagation of thrust) and ramp step-up angle with respect to the kind of sediment, rate of lithification and rate of compaction.

4. Concluding remarks

In geological settings dominated by subduction or collisional tectonics, syn-tectonic sedimentation supplies basin fills in which unpacked sediments, close to the depositional surface, are commonly subjected to deformation before deep burial and complete lithification. As a consequence, the stratal pattern of shallowly nucleated, thrust-related growth folds depends mainly on sedimentation-uplift (shortening) rates, and also on the physical properties of the syn-tectonic deposits (such as the cohesion and the angle of internal friction) and the lithification rate. Quick lithification processes contribute to the tightened final fold geometry, unlike that of slow lithification processes, which lead to more gently folded geometry. In these settings, gravity and tectonics act simultaneously to control syn-sedimentary structures and the final shape of the overthrust terrains.

Acknowledgements

Grateful thanks for the helpful suggestions and the comments leading to the improvement of the paper are due to S. Mitra and to the anonymous referee. We would also like to thank R.J. Norris for detailed and constructive comments, supportive linguistic improvement and editorial assistance. Work supported with UNIPA (ex MURST 60%) and COFIN 2003, P. Renda funds.

References

Agar, S.M., 1988. Shearing of partially consolidated sediments in a lower trench slope setting, Shimanto Belt, SW Japan. Journal of Structural Geology 10, 21–32.

Allen, J.R.L., 1983. Sedimentary Structures, their Character and Physical Basis, 30, Developments in Sedimentology, 2. Elsevier, Amsterdam, 663pp.

Bray, C.E., Karig, D.E., 1985. Porosity of sediments in accretionary prisms and some implications for dewatering processes. Journal of Geophysical Research 90, 768–778.

Broquet, P., Caire, A., Mascle, G., 1966. Structure et evolution de la Sicile occidentale (Madonie et Sicani). Bulletin Societe Géologique France 7(8), 994–1013.

Buckley, D.E., Grant, A.C., 1985. Fault-like features in abyssal plain sediments: possible dewatering structures. Journal of Geophysical Research 90, 9173–9180.

Carson, B., Berglund, P.L., 1986. Sediment deformation and dewatering under horizontal compression: experimental results. Memoirs of Geological Society of America 166, 135–150.

Catalano, R., D'Argenio, B., 1982. Schema geologico della Sicilia. In: Catalano, R., D'Argenio, B. (Eds.), "Guida alla Geologia della Sicilia Occidentale", Guide Geologiche Regionali, 24. Memorie Società Geologica Italiana, Suppl. A, pp. 9–41.

Catalano, R., Franchino, A., Merlini, S., Sulli, A., 2000. Central western Sicily structural setting interpreted from seismic reflection profiles. Memorie Società Geologica Italiana 55, 5–16.

Davison, I., 1987. Normal fault geometry related to sediment compaction and burial. Journal of Structural Geology 9, 393–402.

Farrell, S.G., Eaton, S., 1987. Slump strain in the Tertiary of Cyprus and the Spanish Pyrenees. Definition of paleoslope and models of soft sediment deformation. In: Jones, M.E., Preston, R.M.F. (Eds.), Deformation of Sediments and Sedimentary Rocks, Special Publication of the Geological Society of London, 29., pp. 181–196.

Farrell, S.G., Eaton, S., 1988. Foliations developed during slump deformation of Miocene marine sediments, Cyprus. Journal of Structural Geology 10, 567–576.

Ford, M., Williams, E.A., Artoni, A., Verges, J., Hardy, S., 1997. Progressive evolution of a fault-related fold pair from growth strata geometries, Sant Llorenc de Morunys, SE Pyrenees. Journal of Structural Geology 19, 413–441.

Gill, W.D., Kuenen, P.H., 1958. Sand volcanoes in slumps in the Carboniferous of Co. Clare, Eire. Quarterly Journal of the Geological Society of London 113, 414–460.

Grandjacquet, C., Mascle, G., 1978. The structures of the Ionian Sea, Sicily and Calabria–Lucania. In: Nairn, A.E.M., Kanes, W.H., Stheli, F.G. (Eds.), The Western Mediterranean, 4B. Plenum Press, New York, pp. 257–329.

Hardy, S., Poblet, J., 1995. The velocity description of deformation. 2. Sediment geometries associated with fault-bend and fault-propagation folds. Marine and Petroleum Geology 12, 165–176.

Hardy, S., Poblet, J., McClay, K., Waltham, D., 1995. Mathematical modelling of growth strata associated with fault-related fold structures. In: Buchanan, P.G., Nieuwland, D.A. (Eds.), Modern Developments in Structural Interpretations, Validation and Modelling, Geological Society of London Special Publication, 99., pp. 265–282.

von Huene, R.E., 1984. Tectonic processes along the front of modern convergent margins. Earth Planetary Science Letters 12, 359–381.

Lickorish, W.H., Grasso, M., Butler, R.W.H., Argnani, A., Maniscalco, R., 1999. Structural styles and regional tectonic sting of the "Gela Nappe" and frontal part of the Maghrebian thrust belt in Sicily. Tectonics 18(4), 669–685.

Lowe, D.R., Lo Piccolo, R.D., 1974. The characteristics and origins of dish and pillar structures. Journal of Sedimentary Petrology 44, 484–501.

Maltman, A.J., 1984. On the term "soft-sediment deformation". Journal of Structural Geology 6, 589–591.

Maltman, A.J., 1994. The Geological Deformation of Sediments, Chapman and Hall, London.

Medwedeff, D., 1989. Growth fault-bend folding at southeast Lost Hills, San Joaquin Velley, California. American Association of Petroleum Geologists Bulletin 73, 54–67.

Mills, P.C., 1983. Genesis and diagnostic value of soft-sediment deformation structures—a review. Sedimentary Geology 35, 83–104.

Mitra, S., 1990. Fault-propagation folds: geometry, kinematic evolution and hydrocarboon traps. American Association of Petroleum Geologists Bulletin 74, 921–945.

Morris, J.H., 1979. Lower Paleozoic soft-sediment deformation structures in the western end of the Longford-Down inlier, Ireland. In: Harris, A.L., Holland, C.H., Leake, B.E. (Eds.), The Caledonides of the British Isles, Special Publication of the Geological Society of London, 8., pp. 513–516.

Mosar, J., Suppe, J., 1992. Role of shear in fault-propagation folding. In: McClay, K.R., (Ed.), Thrust Tectonics, Chapman and Hall, London, pp. 921–945.

Mount, V.S., Suppe, J., Hook, S., 1990. A forward modelling strategy for balancing cross section. American Association of Petroleum Geologists Bulletin 74, 521–531.

Nigro, F., Renda, P., 2000. Un modello di evoluzione tettono-sedimentaria dell'avanfossa neogenica siciliana. Bollettino Società Geologica Italiana 119, 667–686.

Ogniben, L., 1960. Nota illustrativa dello schema geologico della Sicilia nord-orientale. Rivista Mineraria Siciliana 64–65, 184–212.

Owen, G., 1995. Soft-sediment deformation in upper Proterozoic Torridonian sandstones (Applecross Formation) at Torridon, northwest Scotland. Journal of Sedimentary Research A65, 495–504.

Roure, F.D., Howell, G., Muller, C., Moretti, I., 1990. Late Cenozoic subduction complex of Sicily. Journal of Structural Geology 12(2), 259–266.

Scandone, P., Giunta, G., Liguori, V., 1974. The connection between Apulia and Sahara continental margins in the Southern Apennines and in Sicily. Memorie Società Geologica Italiana 13, 317–323.

Schlanger, S.O., Douglas, R.G., 1974. The pelagic ooze–chalk–limestone transition and its implication for marine stratigraphy. In: Hsu, K.J., Jenkins, H.C. (Eds.), Pelagic Sediments: on Land and Under the Sea, IAS Special Publication, 1., pp. 117–148.

Schmoker, J.W., Halley, R.B., 1982. Carbonate porosity versus depth: a predictable relation for South Florida. American Association of Petroleum Geologists Bulletin 66, 2561–2570.

Shanmugam, G., Lehtonen, L.R., Straume, T., Syvertsen, S.E., Hodgkinson, R.J., Skibeli, M., 1994. Slump and debris-flow dominated upper slope facies in the Cretaceous of the Norwegian and northern North Sea (61–67°N): implications for sand distribution. American Association of Petroleum Geologists Bulletin 78, 910–937.

Shaw, J.H., Suppe, J., 1994. Active faulting and growth folding in the eastern Santa Barbara Channel, California. Geological Society of America Bulletin 106, 607–626.

Storti, F., Poblet, J., 1997. Growth stratal architectures associated to decollement folds and fault-propagation folds. Inferences on fold kinematics. Tectonophysics 282, 353–373.

Suppe, J., 1983. Geometry and kinematics of fault-bend folding. American Journal of Science 283, 684–721.

Suppe, J., Medwedeff, D.A., 1984. Fault-propagation folding. Geological Society of America Program with Abstracts 16, p. 670.

Suppe, J., Medwedeff, D.A., 1990. Geometry and kinematics of fault-propagation folding. Eclogae Geologica Helveticae 83, 409–454.

Suppe, J., Chou, G.T., Hook, S.C., 1992. Rates of folding and faulting determined from growth strata. In: McClay, K.R., (Ed.), Thrust Tectonics, Chapman and Hall, London, pp. 105–121.

Suppe, J., Sabat, F., Munoz, J.A., Poblet, J., Roca, E., Verges, J., 1997. Bed-by-bed fold growth by kink-band migration: Sant Llorenc de Morunys, eastern Pyrenees. Journal of Structural Geology 19, 443–461.

Tobisch, O.T., 1984. The development of foliation and fold interference patterns produced by sedimentary processes. Geology 12, 441–444.

Torrente, M.M., Kligfield, R., 1995. Modellizzazione predittiva di pieghe sinsedimentarie. Bollettino Società Geologica Italiana 114, 293–309.

Waltham, D., 1992. Mathematical modelling of sedimentary basin processes. Marine and Petroleum Geology 9, 265–273.

Woodcock, N.H., 1976. Structural style in slump sheets, Ludlow series, Powys, Wales. Journal of the Geological Society of London 132, 399–415.

Zapata, T.R., Allmendinger, R.W., 1996. Growth stratal records of instantaneous and progressive limb rotation in the Pre-cordillera thrust belt and Bermejo basin, Argentina. Tectonics 15, 1065–1083.

Zoetemeijer, R., Cloetingh, S., Roure, F., Sassi, W., 1992. Stratigraphic and kinematic modelling of thrust evolution, northern Apennines, Italy. Geology 20, 1035–1038.